Proc. 7th PTTI Planning Meeting,
Washington, D.C., December 1975,
pp. 143-159.

A PORTABLE RUBIDIUM CLOCK FOR PRECISION TIME TRANSPORT

Helmut Hellwig and A. E. Wainwright
National Bureau of Standards
Frequency & Time Standards Section
Boulder, Colorado 80302

ABSTRACT

Based on a commercially available rubidium standard the National Bureau of Standards (NBS) developed a portable rubidium clock. Technical modifications which reduce the sensitivity against temperature, magnetic environment, and barometric changes allow stabilities in the 10^{-12} range under typical clock transport conditions. Under laboratory conditions the clock shows a best stability of 3 parts in 10^{14} . Clock packages based on sealed lead-acid batteries featuring a total weight of 21 kg and 18 hours battery operation were tested; an improved clock package was realized using silver-zinc batteries with 11 kg weight and 28 hours battery operation. Reports of several clock trips to the U.S. Naval Observatory and of one clock trip each to the Bureau International de l'Heure in Paris and to the Hewlett-Packard Company in Santa Clara, California are reported. Time transport precisions of .02 μs have been obtained. Special aspects of the clock modifications and the operating characteristics are discussed, as well as an optimal use of the data of a clock round-trip.

INTRODUCTION

For time comparisons with precisions of better than a few μs between distant locations, cesium clocks are used exclusively at present. The use of these devices is not without constraints due to their size as well as their relatively high power demands. For example, with reasonable and portable battery power supplies cesium clocks must be powered from outlets on the airplane on any transcontinental or intercontinental trip and the purchase of a separate seat is necessary. As a result, cesium clocks not only pose cost and logistics problems, but also affect the reliability of time comparisons. Commercial cesium clocks are under development which promise reduction of the above problems; nevertheless,it appeared prudent to explore the possibilities of small commercially available rubidium standards which offer the potential of very small clock packages. Even mailable clocks appear feasible.

THE BASIC RUBIDIUM STANDARD

Small rubidium standards are now commercially available. A unit was selected featuring about 1 ℓ volume (approximately 10 x 10 x 10 cm) and a weight of about 1 kg. The basic stability of the clock was measured and the results are depicted in fig. 1. The frequency stability of the clock can be described by* $\sigma_y(\tau) = 6 \times 10^{-12}\tau^{-1/2}$, a flicker floor of 3×10^{-13}, and a long term stability of about 3×10^{-12} at τ = 1 day. For time transport with a precision of 0.1 μs the frequency stability requirement can be stated as $\sigma_y(\tau=T) < 10^{-7}\ T^{-1}$, where T is the interval in seconds between the time comparison at two remote locations (trip time). From this equation and fig. 1 it is clear that the rubidium clock is basically capable of providing time comparisons to better than 0.1 μs for trip times out to many hours. It is therefore obvious that environmental effects are of primary concern. For long clock trips possible frequency drifts could be significant. Clock trips take typically less than 18 hours. Environmentally induced frequency changes should therefore be individually in the 10^{-12} range, or they should be calculable.

On a trip the clock encounters three major environmental changes: a) magnetic field; b) temperature; c) barometric pressure. The performance of the particular NBS unit was tested against these changes. For atomic frequency standards, frequency changes due to repositioning are principally magnetic field effects. The performance of the unit under test was: a) position (magnetic field): 1.2×10^{-10} worst case in the earth magnetic field; i.e., strongly dependent on the particular position or orientation. b)temperature: about 7×10^{-12} per °C in the range of 26-40 °C baseplate temperature; c)barometric pressure, parts in 10^9 from atmospheric pressure to vacuum. It was suspected that the barometric effect was related to temperature, in particular, temperature gradient effects, and that the barometric sensitivity would be much less around atmospheric pressure.

* $\sigma_y(\tau)$ is the square root of the two sample variance of fractional frequency fluctuations. τ is the sample time measured in seconds.

We therefore decided to reduce only the magnetic field and temperature sensitivity and trust that the barometric sensitivity around atmospheric pressure would pose no major problems.

In view of the need to provide the clock with a portable battery power pack the sensitivity of the frequency against supply voltage changes was of interest. Figure 2 shows this sensitivity which can be described by about 5×10^{-12} per volt. Therefore, only a relatively conventional voltage regulation was necessary if batteries with a flat discharge voltage characteristic were to be used, such as lead-acid or silver-zinc. Strongly varying voltages under discharge, such as featured by alkaline batteries, would cause non-trivial problems.

THE IMPROVED CLOCK

The existing outer magnetic shield of the unit was partially reworked. The shield was repositioned to allow at least seven millimeter distance everywhere to the inner shield, especially at the critical location of the photo detector. Also, adequate overlaps between the joining portions of the shield were introduced. A third magnetic shield was added and the space between the second and third shield was filled with foam. This latter measure highly reduces convective cooling of the unit and forces the mounting (baseplate) to act as the only significant heat sink. This reduces temperature gradients within the unit which would depend on the state of air circulation around the unit and affect frequency stability and frequency accuracy. The baseplate configuration, i.e., the layers of magnetic shields and the baseplate itself, were joined using heat conductive paint. The only openings in the outer magnetic shield are those for the wires of the necessary supply and control voltages and a small hole to provide access to the tuning capacitor of the crystal oscillator. To "harden" the unit against acceleration and vibration, all critical wires and components were glued to the circuit board, also, the adjustment potentiometer for the magnetic field current was replaced by a fixed resistor providing an offset from the nominal frequency of several parts in 10^{11}

I BAROMETRIC SENSITIVITY

BOULDER ⟶ SEA LEVEL
(~0.8 atm) (~1.0 atm)

(a) ORIGINAL UNIT + $1.5X10^{-11}$

(b) SEALED UNIT < + $2X10^{-12}$

II MAGNETIC FIELD SENSITIVITY
(ORIENTATION IN EARTH'S FIELD)

(a) ORIGINAL UNIT $1.2X10^{-10}$ WORST CASE

(b) SHIELDED UNIT $3X10^{-12}$ WORST CASE

TABLE 1

TEMPERATURE COMPENSATION
VIA C-FIELD CURRENT ADDITION
(TEST-RANGE: 26°C TO 40°C AT BASEPLATE)

R(Ω)	1.5K	613	580	562
$\Delta\nu/\nu$ (10^{-12}) PER C	+7.2	+1.7	-0.14	-0.8

TABLE 2

The magnetic field sensitivity under the worst possible orientation in the earth's magnetic field was reduced by the measures described above to 3×10^{-12} total frequency change as shown in Table 1. The commercial rubidium standard features temperature compensation using current addition into the internal magnetic field current supply. This additional current is controlled by a temperature sensor, i.e., the atomic frequency is changed magnetically to compensate for temperature induced frequency shifts. In a series of temperature tests from 26 °C to 40 °C at the baseplate an optimum adjustment for the controlling resistor was experimentally found. The unit was mounted on a heavy plate which was temperature stabilized using a commercial temperature controller. These tests were carried out with the complete unit featuring the new third magnetic shield as described above with wires leading out of the unit to allow quick substitution of the resistor. Table 2 gives the result for four different resistors. 1.5 k was the original value supplied by the manufacturer. We can see that the temperature sensitivity could be reduced by a factor of about 50 by choosing a resistor of 580 Ω.

Finally the unit was barometrically sealed using epoxy glue to close the small gaps in the outer magnetic shield. Thus, the outer magnetic shield serves as a pressure container. Though this action highly reduces the effects of barometric pressure changes (except for residual flexing of the walls of the magnetic shield under pressure changes), it introduces a pressure problem via temperature fluctuation inside of the sealed case. The pressure will change by the same percentage by which (absolute) temperature changes occur. Nevertheless, an advantage can be gained since barometric pressure changes of the order of 10% are encountered during typical transport conditions whereas temperature changes, i.e., temperature induced pressure changes, of the order of one percent are encountered. Especially in a laboratory environment improvements were expected to be significant since the temperature is stable to a fraction of a percent whereas barometric pressure changes due to weather related effects can be very significant and be up to many percent.

Figure 3 demonstrates this dramatically. Curve A in fig. 3 depicts the performance of the unit with all modifications installed except for the barometric sealing. We see that the flicker level has substantially dropped, and that the long-term stability (now 1×10^{-13} for $\tau = 1$ day) has improved as compared to fig. 1. A reliable measurement of the drift performance of the unit could be done. The drift was typically 1×10^{-13}/day, or less during a period of many months.* The barometric sealing lowered the flicker floor to about 3×10^{-14}, which we believe is the best stability ever measured with a rubidium standard. Table 1 shows the reduction in barometric sensitivity for a change from 0.8 atm to 1.0 atm corresponding to going from Boulder Colorado to sea level. The original unit, with all improvements except for barometric sealing, showed a change of 1.5×10^{-11}. The sealed unit showed an effect of less than 2×10^{-12}.

The improved rubidium frequency standard is mounted with its baseplate inside an aluminum carrying case, thus securing adequate cooling. The output of the standard is normally 10 MHz. A divider provides externally available 5 MHz and 1 pulse/s outputs. Both outputs are buffered and can handle 50 Ω loads with a 1 volt rms signal for 5 MHz, and for the pulse a 5 volt peak with 10 ns rise time. A battery power pack was installed inside the case with a diode disconnect circuit. A regulated power supply, switchable for 115 and 230 V, supplies the standard and the divider circuit if the unit is plugged into the power line. Thus, no precaution is necessary in connecting or disconnecting from power line service. Both battery and line power supply feed their voltages to the standard via a 24.3 V regulator.

---

* During several days following a clock trip, the actual performance is somewhat worse than the performance depicted in fig. 3.

The first battery pack used was a sealed lead-acid type which gave the total unit a weight of 21 kg and 18 hours battery life. The weight of this unit caused difficulties in handling as carry-on luggage on airplanes. Therefore, the lead-acid batteries were replaced by silver-zinc batteries, giving the unit a total weight of 11 kg and 28 hours battery life. This battery pack feeds about 31 V into the regulator during most of the discharge with a somewhat higher voltage during the first half hour and a rapid voltage drop at the end of the charge life.

Initially, the silver-zinc batteries were charged from a built-in power supply. Unfortunately, this solution did not stand up to actual service and we had to go to external charging. The principal reason for this is the peculiar charge and discharge characteristic of silver-zinc batteries and a change of this characteristic with time due to a mismatch between battery type and charge current.* The principal feature of the power supply is that it must disconnect totally any charge current from the batteries when the batteries are fully charged because a trickle charge would lead to destruction of the silver-zinc batteries. It also has a total cut-off feature which disconnects the batteries from the standard if the battery voltage drops below a preset level. This stops the clock, but protects the batteries which would otherwise be destroyed. We plan to replace the present battery set by a "low current" style which will allow us to use the built-in automatic charging supply.

Figure 4 shows a photo of the complete unit. A meter is provided in the unit with six switchable positions which allow the reading of the regulator input voltage, the regulator output voltage, the battery voltage, the battery charge-discharge current, the crystal oscillator servo voltage in the standard, and the light intensity monitor voltage in the standard. Also, a lock indication is provided.

---

* The silver-zinc batteries will be gradually destroyed if charged by a too low current. Our type of battery was a "high current" design (unknown to us) and demanded > 1.5 A charge current, whereas our power supply furnished about 0.3 A.

OPTIMUM USE OF CLOCK TRIP DATA

A definition of clock transport conditions and terms is given in fig. 5. Clock transport occurs from A to B and, if possible, back to A. The time elapsed on the trip from A to B is T_{AB} and correspondingly the time from B to A is T_{BA}. The actual time spent by the clock at location B is T_B. The change in the time reading of the clock at location B with respect to the clock at B is Δt_{BB}. The so-called "closure" is Δt_{AA}, i.e., the difference of the clock reading when it returns to location A with respect to the clock at A.

The most simple assessment of a clock trip would make use only of Δt_{AA}. An assessment of the error or uncertainty of the clock comparison is then the difference between the measurement value of Δt_{AA} and the value for Δt_{AA} as predicted from the rate of the clock at A before leaving. In a round-trip, however, more data are usually available and can be used to arrive at a better estimate of the time differences of the clocks at A and B. Figure 6 illustrates this. Plotted are the fractional frequency offsets y of the portable clock as a function of real time at the various locations and during the trip. The clock has an average rate y_A' at location A before it leaves. If B is also a time-keeping laboratory with high-performance standards, i.e., clock A and clock B are at about the same rate, then a precise reading of the portable clock frequency at B can be made leading to the value y_B ($y_B = \Delta t_{BB}/T_B$). Upon return to A the clock will show the frequency y_A'' which usually is not significantly different from the original rate y_A'. The average frequency for the combined trip time T_{AB} and T_{BA} can then be calculated from the following equation

$$y_B^A = \frac{\Delta t_{AA} - \Delta t_{BB}}{T_{AB} + T_{BA}} .$$

This equation is, of course, only accurate to the degree of validity of the measurement of Δt_{BB} or y_B. In other words we have to assume that the frequency or rate of the clocks at location B is not much different than those at A. This requirement is not too stringent because the requirement on our knowledge of the clocks at B in fractional frequency is the same as our requirement on the frequency of the portable clock during the trip time. Since 10^{-12} corresponds to 0.1μs in about 1 day trip time, a knowledge of the frequency of the clocks at B to 1×10^{-12} is totally adequate for most clock trip purposes. In fact, for precision time laboratories this is a near trivial requirement because typically the rate is known to much better than 1×10^{-12}.

y_B^A can then be used to predict the time reading of laboratory A at the time of arrival of the portable clock at B and the reading of laboratory B at the time of arrival of the clock back in laboratory A. The time difference between laboratory A and B for the first leg of the clock trip is $(t_A - t_B)_{AB}$, and it is $(t_A - t_B)_{BA}$ for the second leg of the clock trip. A change in clock behavior and/or in the two trip conditions would cause an error term. Obviously the error term can be estimated from the difference Δt_B^A, of the time readings between laboratories A and B obtained from the two legs of the clock trip. The following equation gives an estimate of the error of Δt_B^A.

$$\delta \Delta t_B^A \simeq |(t_A - t_B)_{AB} - (t_A - t_B)_{BA}| + \text{const.}$$

Of course the first term in the equation will tend to be non-zero if there is a rate difference between clocks A and B. If the rate difference is significant, it should be accounted for before the error assessment. In this equation we added a constant since the difference in the time differences could be small fortuitously. Thus the constant includes an estimate of the fundamental stability performance of the clock (excluding trip induced frequency changes), as well as an estimate of the uncertainty in the rates of clocks at A and B if the two legs of the clock trip are far apart in time. If only one leg of the clock trip is successful an improved estimate of $(t_A-t_B)_{AB}$ or $(t_A-t_B)_{BA}$ and the associated error $\delta\Delta t_B^A$ can still be made using the clock rates y_B at B and y_A' and/or y_A'' at A.

CONCLUSIONS

A list of clock trips carried out during 1975 is given in Table 3. Four clock trips were done to the U. S. Naval Observatory in Washington, DC; two of which were complete round-trips. One trip was carried out to the Bureau International de l'Heure (BIH). This was only a one-way trip since the return trip was not usable because of problems due to shorting batteries. Finally, a trip to the Hewlett-Packard Company was carried out. This trip was a round-trip; however, the data from the return trip were not used due to a servo system problem in the rubidium standard itself. The first trip to the USNO in May 1975 featured the clock package with lead-acid batteries. All other clock trips were made with the silver-zinc battery. The table gives the approximate trip time in hours and the measured time difference between the time scale of the laboratories and UTC(NBS). Finally, the last column gives the estimated uncertainty of the time comparison.

The use of all available data from measurements at laboratories A and B allows a reduction in the uncertainty of the time measurement. The clock package is small enough that it could be shipped by priority air freight. On trips within the US and to Europe we never did encounter any serious difficulties with the clock being handled as carry-on luggage; not even the airport security posed any significant problems. Modifications of the battery package are obvious. For shorter trips of up to several hours, lead-acid batteries may still be the correct choice because of their comparative cheapness and reliability. If weight counts and short clock trips are only envisioned, then a small silver-zinc battery may be used with advantage reducing the weight by an additional several kg. A larger battery is possible for up to forty hours of battery operation increasing the weight of the portable clock to not more than 15 kg.

ACKNOWLEDGMENTS

The authors wish to acknowledge the help extended to them by the staffs of the cooperating laboratories: BIH, USNO, Hewlett-Packard and NBS. In particular, we wish to acknowledge the help in data taking and analysis extended to G. M. R. Winkler of USNO, and D. Allan of NBS. Also, the international clock transport would not have been possible without the cooperation by P. Giacomo of the BIPM, J. J. Gagnepain of the University of Besancon and F. Addor of Ebauches, S. A.

CLOCKTRIPS

DESTINATION	DATE (RANGE)	T_{AB} (h)	T_{BA} (h)	$(UTC)_i-(UTC)_{NBS}$ (μs)	$\delta\Delta t_B^A$ (μs)
USNO	26 MAY 75	6	-	-7.6	0.2
USNO	16/17 JULY 75	8	7	-8.10	0.03
USNO	30/31 JULY 75	7	6	-8.41	0.02
USNO	26/27 SEPT 75	6	-	-8.23	0.03
BIH(OP)	27/28 SEPT 75	18	-	-6.10	0.1
HP	9/21 NOV 75	5	(5)	-2.96	0.05

USNO = US NAVAL OBSERVATORY

BIH(OP) = BUREAU INTERNATIONAL de l'HEURE(PARIS OBSERVATORY)

HP = HEWLETT PACKARD COMPANY

TABLE 3

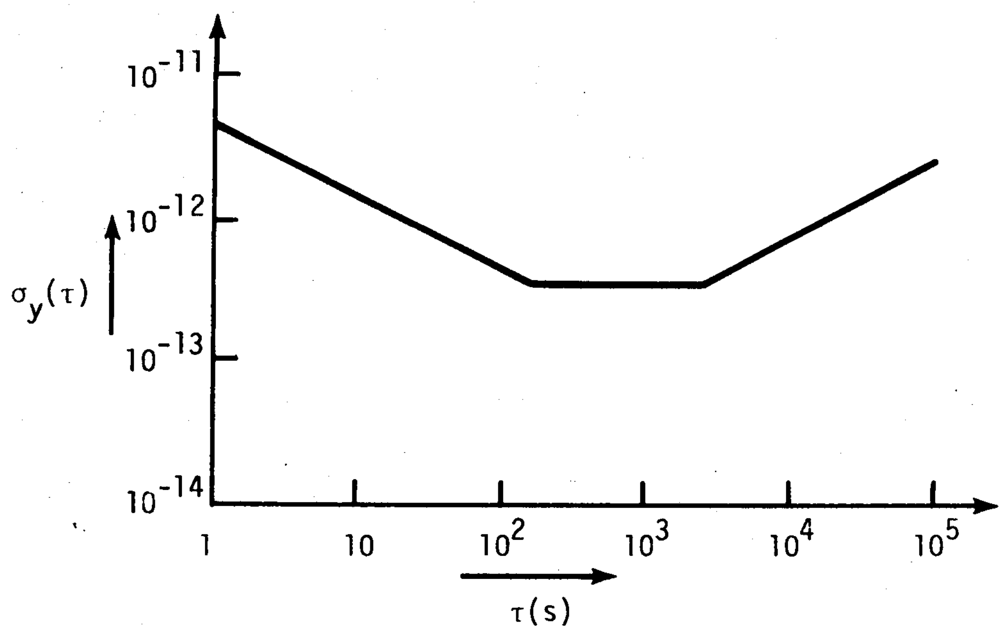

FIGURE 1. Time-Domain Stability of a Commercial Rubidium Standard.

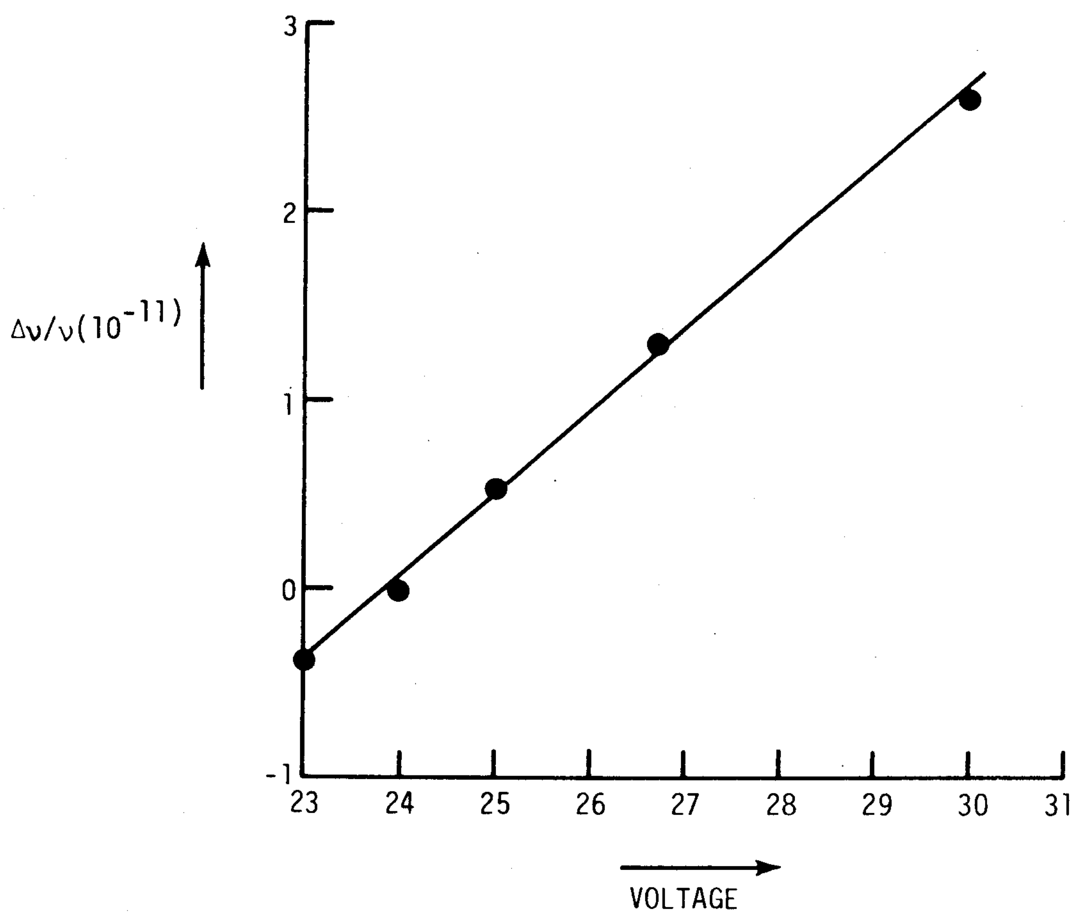

FIGURE 2. Frequency Change as a Function of Supply Voltage for the Commercial Rubidium Standard.

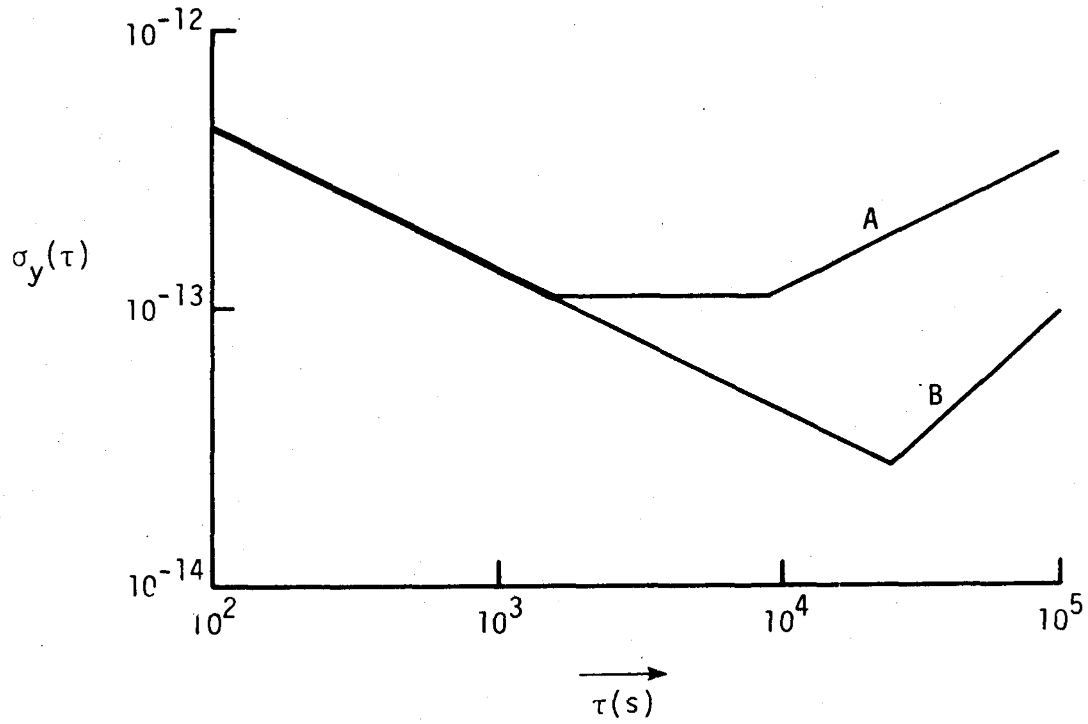

FIGURE 3. Time-Domain Frequency Stability of the Improved Unit.

curve A Improved magnetic shielding and temperature compensation.

curve B Improved magnetic shielding, temperature compensation and barometric sealing.

A frequency drift of approximately 1×10^{-13} per day is removed from the data.

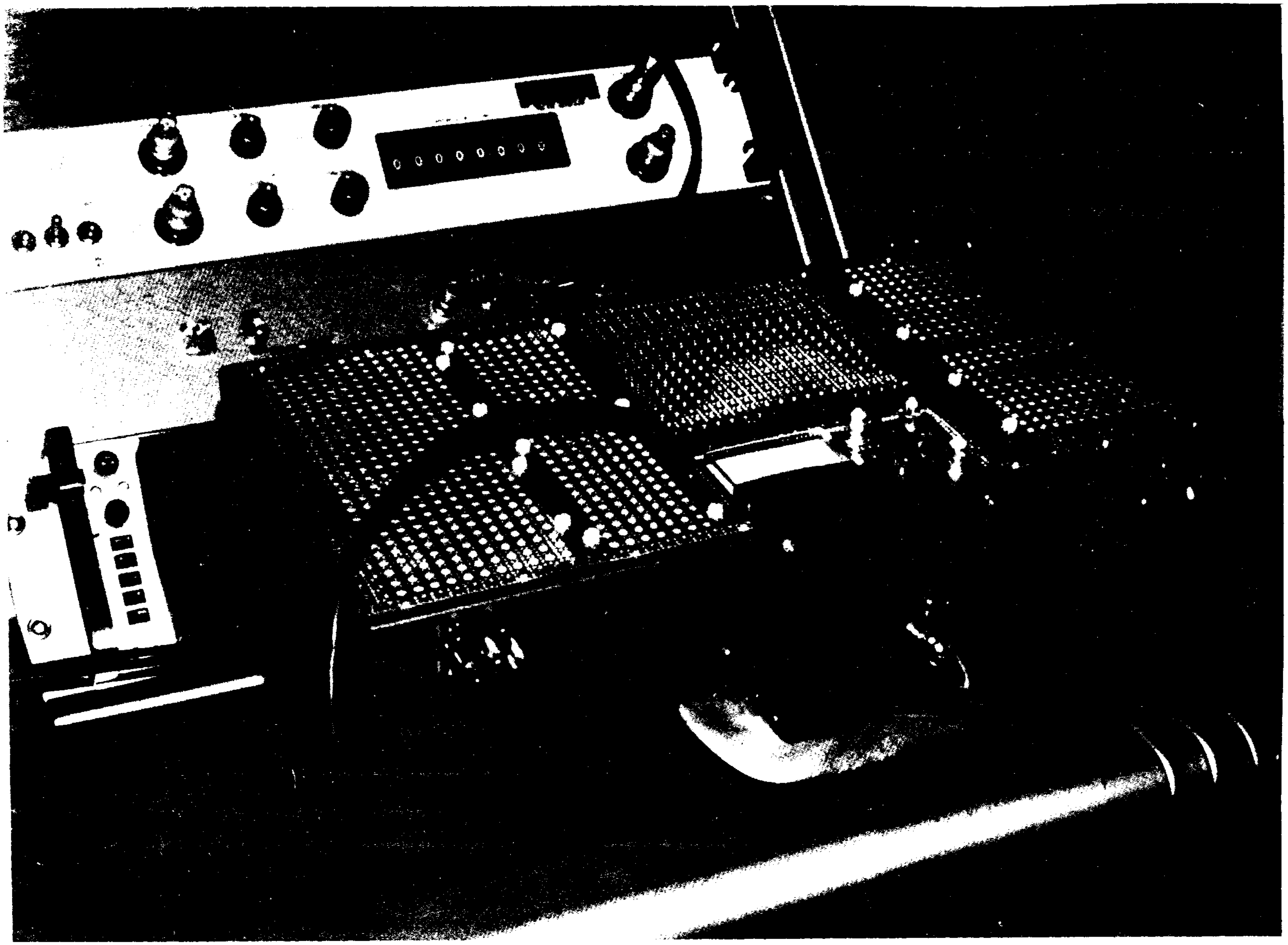

FIGURE 4. Photo of the portable rubidium clock.

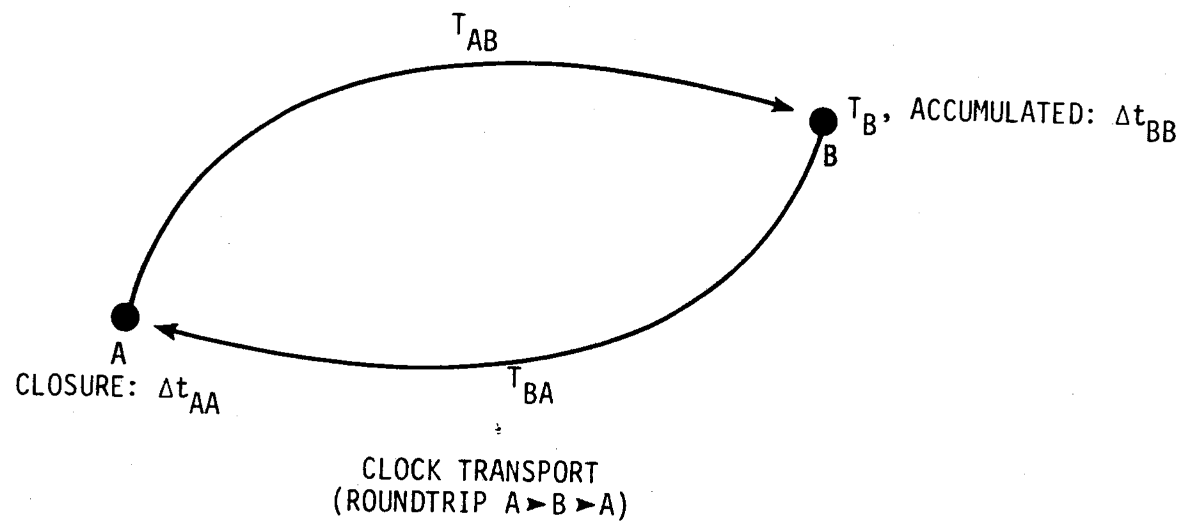

FIGURE 5. Principle of a Round-Trip Clock Transport from Laboratory A to B and Back to A.

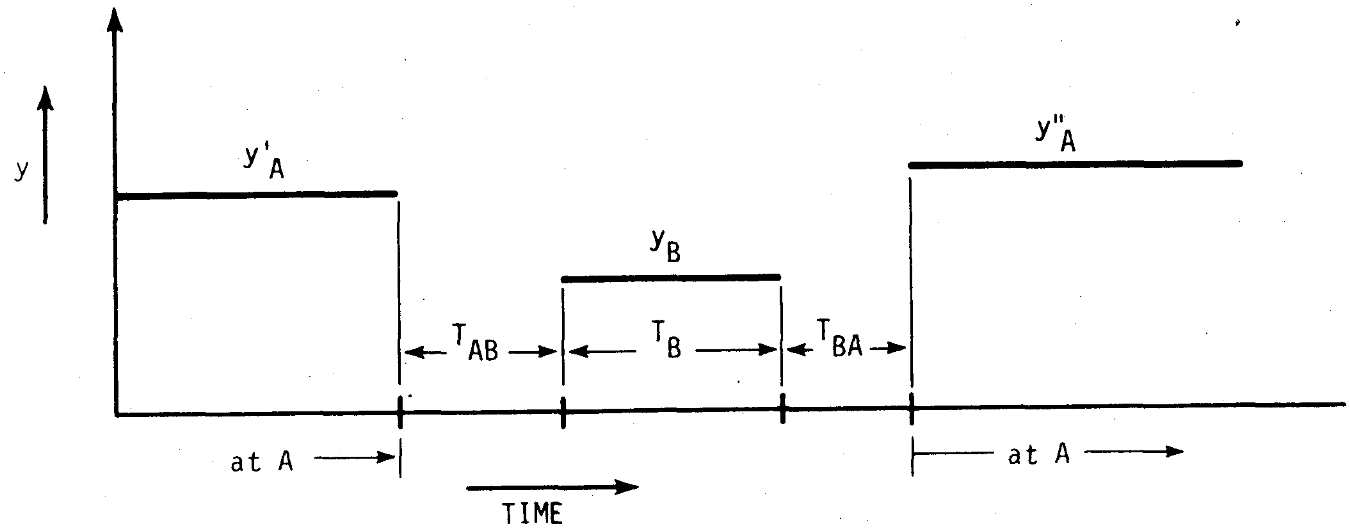

$$y_B^A = \frac{\Delta t_{AA} - \Delta t_{BB}}{T_{AB} + T_{BA}}$$

$$\text{ERROR} \quad \delta\Delta t_B^A \approx \left| (t_A - t_B)_{AB} - (t_A - t_B)_{BA} \right| + \text{CONST}$$

FIGURE 6. Best Use of Data from a Clock Round-Trip.

y = fractional frequency.

T = trip times.

Δt_{AA} = accumulated time reading of the portable clock from leaving A and upon returning to A.

Δt_{BB} = accumulated time reading of the portable clock between arrival and departure at B.

$\delta\Delta t_B^A$ = time error for a clock trip A to B or B to A.